

ON THE NATURE OF GGD 25¹

Joaquín Bohigas

Instituto de Astronomía, UNAM, Ensenada, B.C., México

Received 1991 December 5

RESUMEN

Imágenes en $H\alpha$, [N II] 6584 A y [S II] 6717, 6731 A de la región GGD 25 demuestran de manera concluyente que este no es un objeto Herbig-Haro, sino parte de una región H II. De la imagen en $H\alpha$ se descubrió una estrella en emisión en el campo. Se presenta un mapa bidimensional de la densidad electrónica de una región H II incluida en la imagen.

ABSTRACT

$H\alpha$, [N II] 6584 A and [S II] 6717, 6731 A images conclusively show that GGD 25 is not a Herbig-Haro object, but part of an H II region. An emission line star was discovered from the $H\alpha$ frame. A bidimensional electron density map for an H II region included in these images is presented.

Key words: HERBIG-HARO OBJECTS - NEBULAE-H II REGIONS

I. INTRODUCTION

GGD 25 is one of the nebulae proposed by Gyulbudaghian, Glushkov, & Denisyuk (1978) as a possible Herbig-Haro object due to its morphological appearance and its closeness to a star forming region. This region, NGC 6334, contains several H II regions and is characterized by a high degree of structural complexity and a large variety of young objects: extended infrared emission (McBreen *et al.* 1979; Persi & Ferrari-Toniolo 1982; Harvey & Gaitley 1983; Harvey, Hyland, & Straw 1987; Straw, Hyland, & McGregor 1989), masers (Moran & Rodríguez 1980), bipolar fluxes (Rodríguez, Cantó & Moran 1982, 1988), molecular disks (Jackson, Ho, & Haschick 1988), etc.

Infrared observations of region IV taken at 2.2 and 20 μm (Harvey & Gaitley 1983) reveal an elongated structure aligned in the N-S direction. GGD 25 is located near the maximum of the northern lobe. This bipolar structure is clearly seen at 6-cm, and has been identified as an H II region, NGC 6334 A (Rodríguez, Cantó, & Moran 1988). Based on the coincidental location of GGD 25 with respect to NGC 6334 A, these authors propose that it is not a Herbig-Haro object, but a visible part of the H II region. In this work this hypothesis is appraised comparing images taken at spectral lines

– $H\alpha$, [N II] 6584 A and [S II] 6717, 6731 A – which characterize the nature of a nebular object, i.e., whether it is a reflection nebula, is being excited by a shock, or is being photoionized.

II. OBSERVATIONS AND DATA REDUCTION

Observations were made on May 19, 21 and 22, 1991, at the 2.1-meter telescope of the Observatorio Astronómico Nacional, San Pedro Mártir, with a 384x576 pixel CCD detector. Images at I and 5 interference filters were obtained. Characteristics of the interference filters for an operating temperature of 0°C, as well as the total exposure times are presented in Table 1. The maximum exposure time per frame was 20 minutes. Six frames were obtained with the I filter, with a total exposure time of 6 minutes. Image quality during the three observing

TABLE 1

FILTERS AND EXPOSURE TIMES

λ_0	FWHM	Ion	t(min)
6584	11	[N II]	40
6563	10	$H\alpha$	40
6650	50	Continuum	20
6717	10	[S II]	20
6724	50	[S II]	40
6731	4	[S II]	20

1. Based on observations collected at the Observatorio Astronómico Nacional, San Pedro Mártir, B.C., México.

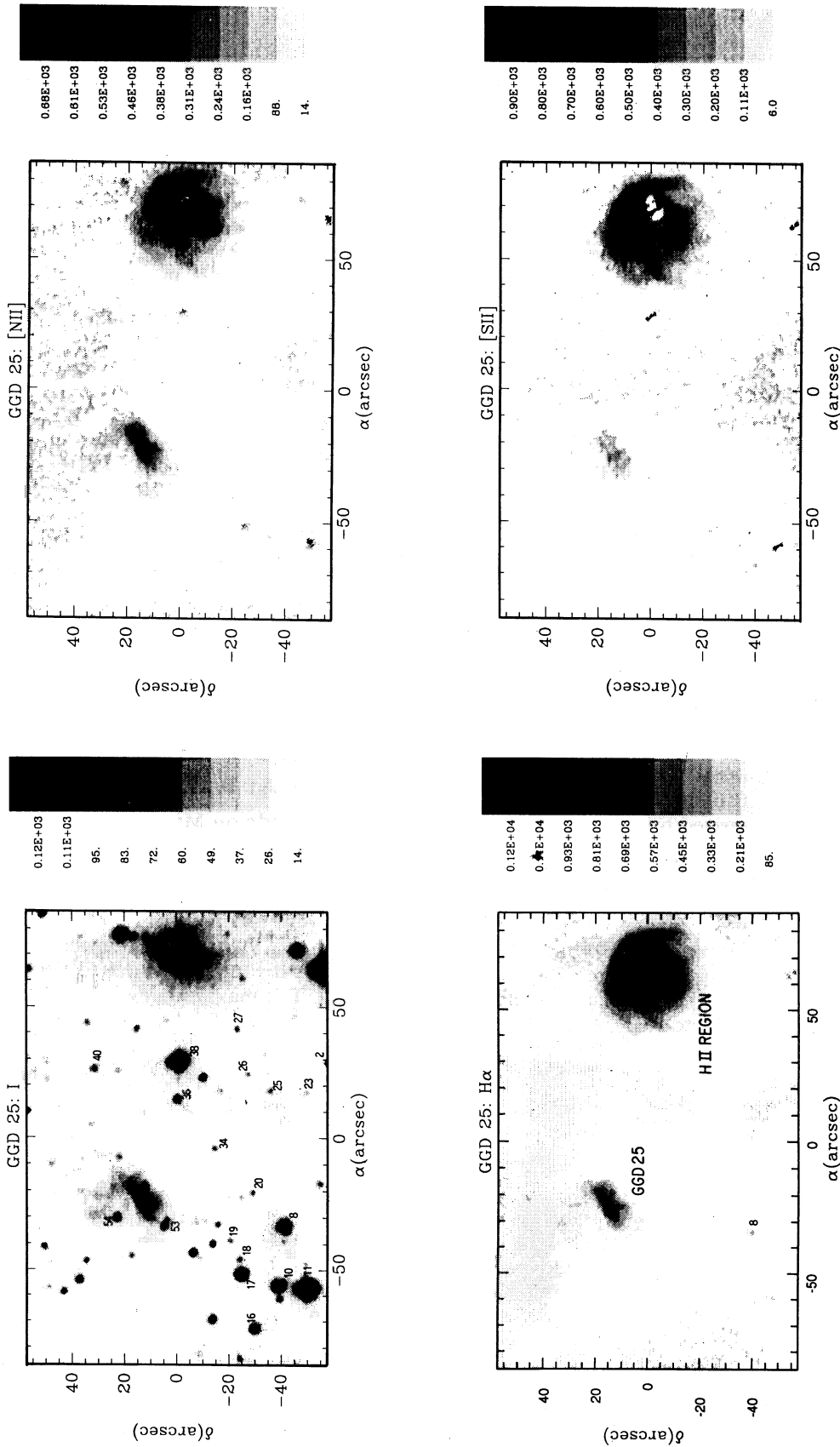


Fig. 1. (a) I filter image of GGD 25. Sources from Harvey, Hyland, & Straw (1987) have been numbered for identification purposes. (b) H α image. Star number 8 can be seen in this frame, indicating that it is an emission line star. (c) [N II] 6584 Å image. (d) [S II] 6717, 6731 Å image.

nights was about 1.6 arcsec. Data reduction was carried out with the IRAF package².

Images of the region in $H\alpha$, $[N II] 6584 \text{ \AA}$, $[S II] 6717, 6731 \text{ \AA}$ and I are presented in Figure 1. A continuum image taken with a filter centered at 6650 \AA was subtracted from the line images. Image calibration was done correcting for the filter bandwidth and assuming that field stars have the same number of counts in all filters, a reasonable assumption considering that central wavelengths differ by not more than 150 \AA . All these images

2. IRAF is distributed by NOAO which is operated by AURA under contract to the NSF.

were degraded with a median filter with a box size equivalent to the image quality.

The former frames were used to produce images of the line ratios $H\alpha/[N II]$ and $H\alpha/[S II]$, shown in Figure 2. Image calibration was performed using the spectral response curves of each filter in order to determine their transmission at the corresponding line wavelength. In the absence of spectroscopic observations of the region, it is difficult to assess the absolute accuracy of these images. Fortunately, the frames contain an H II region located to the west of NGC 6304 A, at $\alpha = 17^h 16^m 49^s$ $\delta = -35^\circ 51' 53''$, with which it was possible to validate the procedure being followed. Relative precision within a given image can be estimated

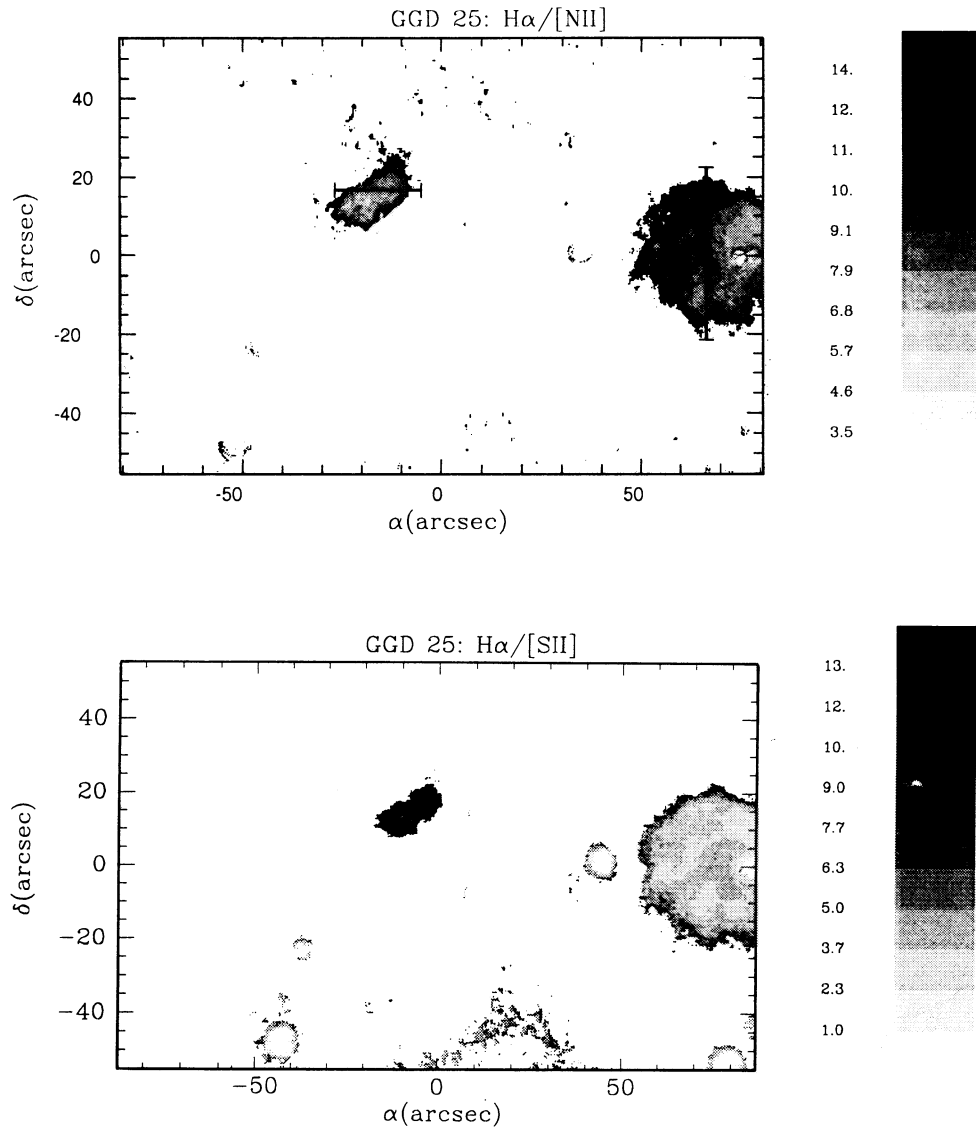


Fig. 2. (a) $H\alpha/[N II]$ line ratio image. (b) $H\alpha/[S II]$ line ratio image.

assuming that the main source of uncertainty is the sky background being subtracted from the source frames (continuum and line images). Error images were produced in this fashion, and used to confine the images for the line ratios, shown in Figure 2, so that the relative accuracy throughout them is better than 20%. Thus, the images for the line ratios are restricted to those pixels in the source frames where signal to noise ratio was roughly larger than 5σ . A detailed description of this procedure is described elsewhere (Bohigas 1991).

Finally, an electron density map for the H II region was created. It was produced from the ratio of the images [S II] 6717, 6731 Å and [S II] 6731 Å and the interpolation formula given by McCall (1984). It is shown in Figure 5, along with the associated error map. Once again, in the absence of spectroscopic information the appraisal

of the absolute accuracy is an awkward question. On the other hand, the interpolation formula is supposed to be accurate to within 5%. Since the determination of the electron density requires additional operations, uncertainties derived from a correct prediction of the sky background in the source images are amplified. Thus, electron densities were estimated only for those pixels where signal to noise ratio was roughly larger than 10σ . Even so, uncertainties on the values for the density are typically larger than 50%, as can be seen from the error map. These errors are more consequential than any possible inaccuracy in the absolute values. Temperature fluctuations shift the transmission curve of an interference filter, an important effect for narrow bandwidths ($< 10 \text{ Å}$), as with the [S II] 6731 Å filter. At the time when the [S II] 6731 Å image was taken the central

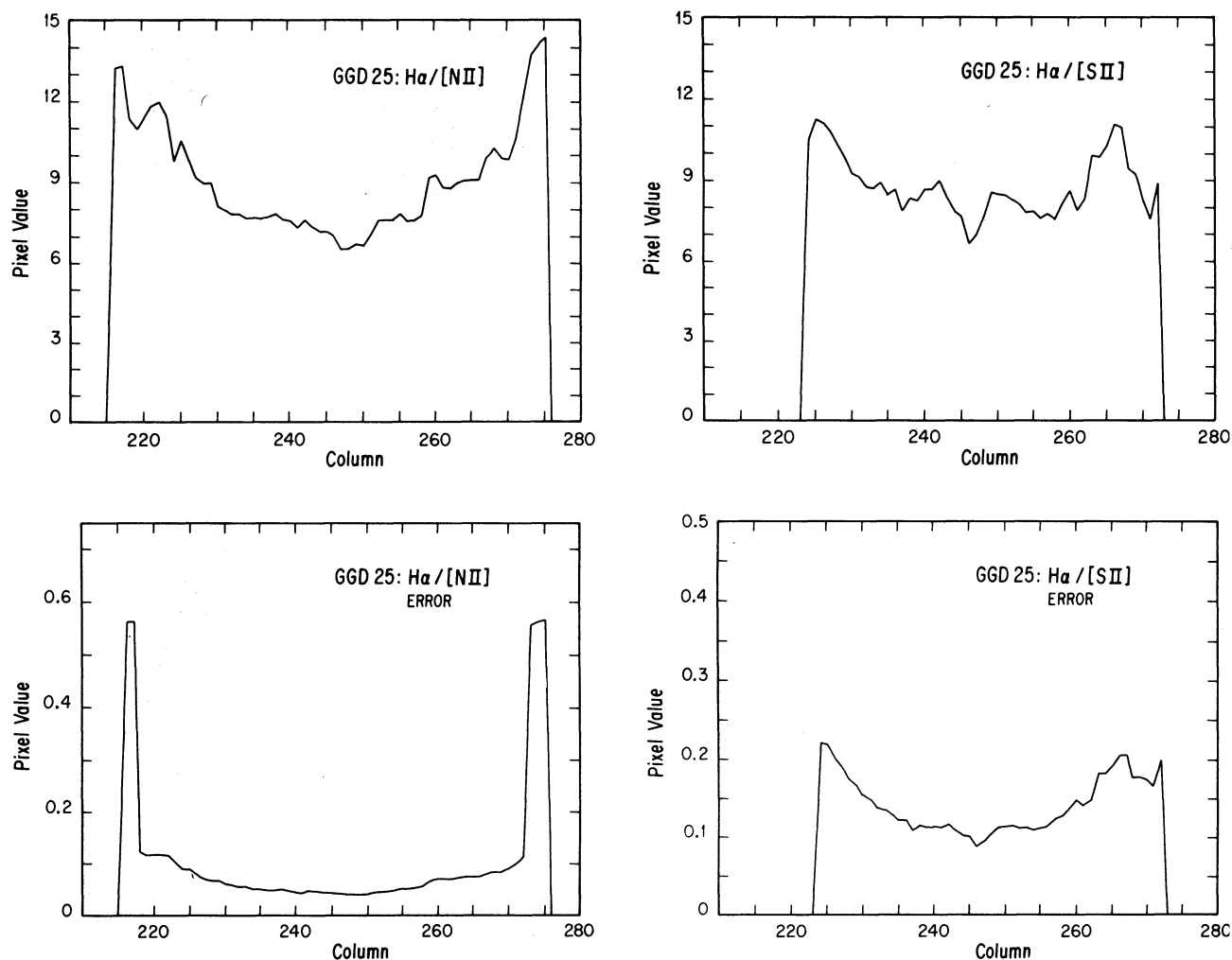


Fig. 3. (a) Scan across GGD 25 for the H α /[N II] line ratio image. Matching errors are shown below. (b) Same as above, for the H α /[S II] line ratio image. The scan position is shown in Figure 2a.

wavelength shift was smaller than 1 Å, and the line was well within the filter's transmission curve.

III. RESULTS

a) Direct Images

As can be seen in Figure 1, GGD 25 is prominent in all the emission lines, though not as bright as the nearby H II region. This suggests that GGD 25 is not a reflection nebula. On the other hand, it is very prominent in I , where the H II region is much more restricted in size. As a matter of fact, GGD 25 can also be seen in the image taken with the continuum filter centered at 6650 Å (not shown here). Polarimetric observations should establish whether the continuum emission is produced *in situ* or is dispersed light.

An unexpected reward from the $H\alpha$ image is the

discovery that source number 8 of Harvey, Hyland, & Straw (1987) is an emission line star. It only appeared in the two $H\alpha$ frames, which were taken at different nights. Thus, variability can be ruled out since the star was absent in those line frames obtained at about the same time as the $H\alpha$ images.

b) Line Ratios

In shock excited regions, such as a Herbig-Haro object, $H\alpha/[N II]$ and $H\alpha/[S II]$ are both close to 1. These ratios are larger than around 4 in a photoionized region. Bow shocks can be an exception to this rule, and can thus introduce some ambiguity to these criteria, since under such a circumstance these line ratios can be similar to those normally found in H II regions (Hartmann & Raymond 1984). Since the morphology of GGD 25 does not suggest the presence of knots where bow shocks

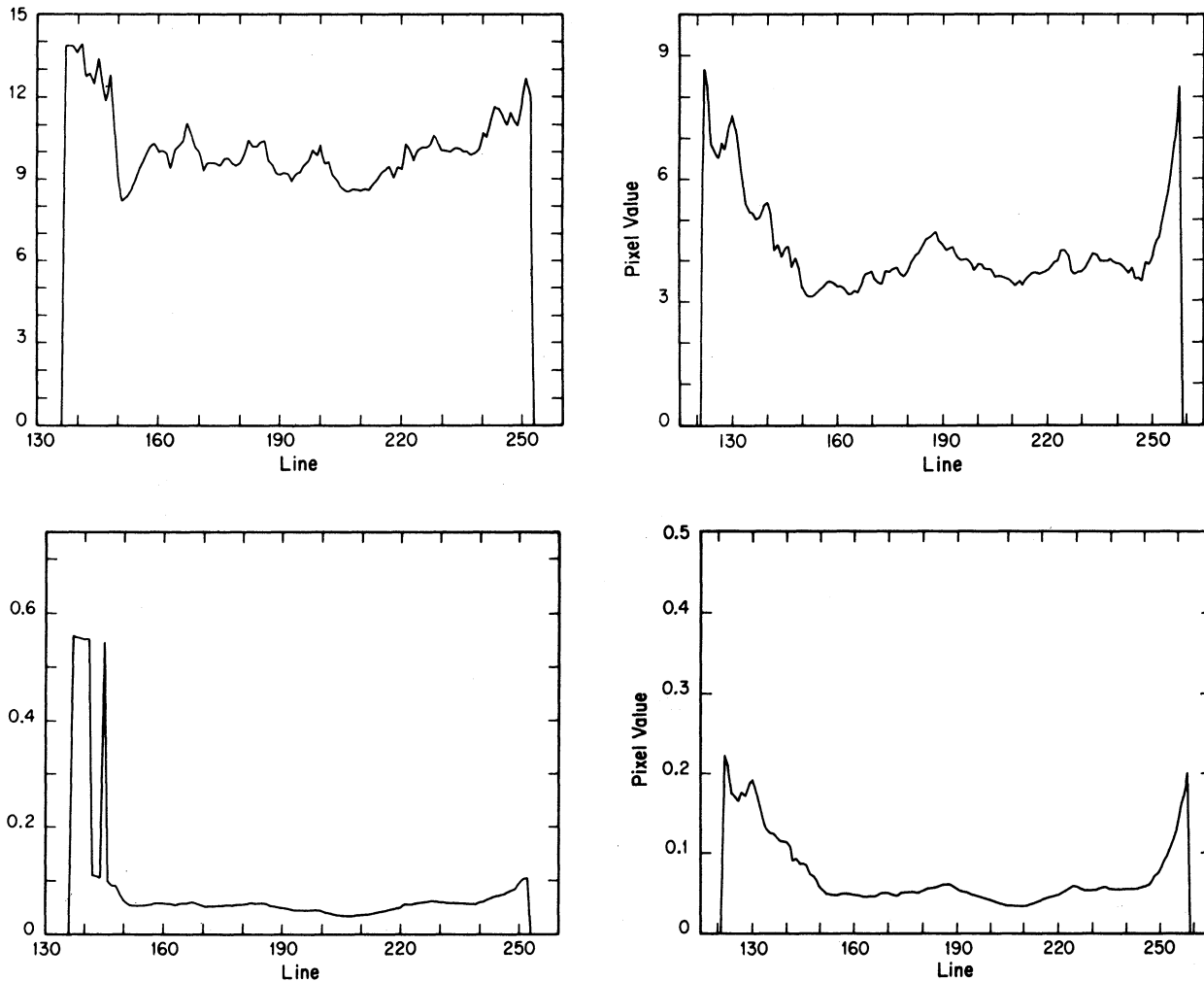


Fig. 4. (a) Scan across the western H II region for the $H\alpha/[N II]$ line ratio image. Matching errors are shown below. (b) Same as above, for the $H\alpha/[S II]$ line ratio image. The scan position is shown in Figure 2a.

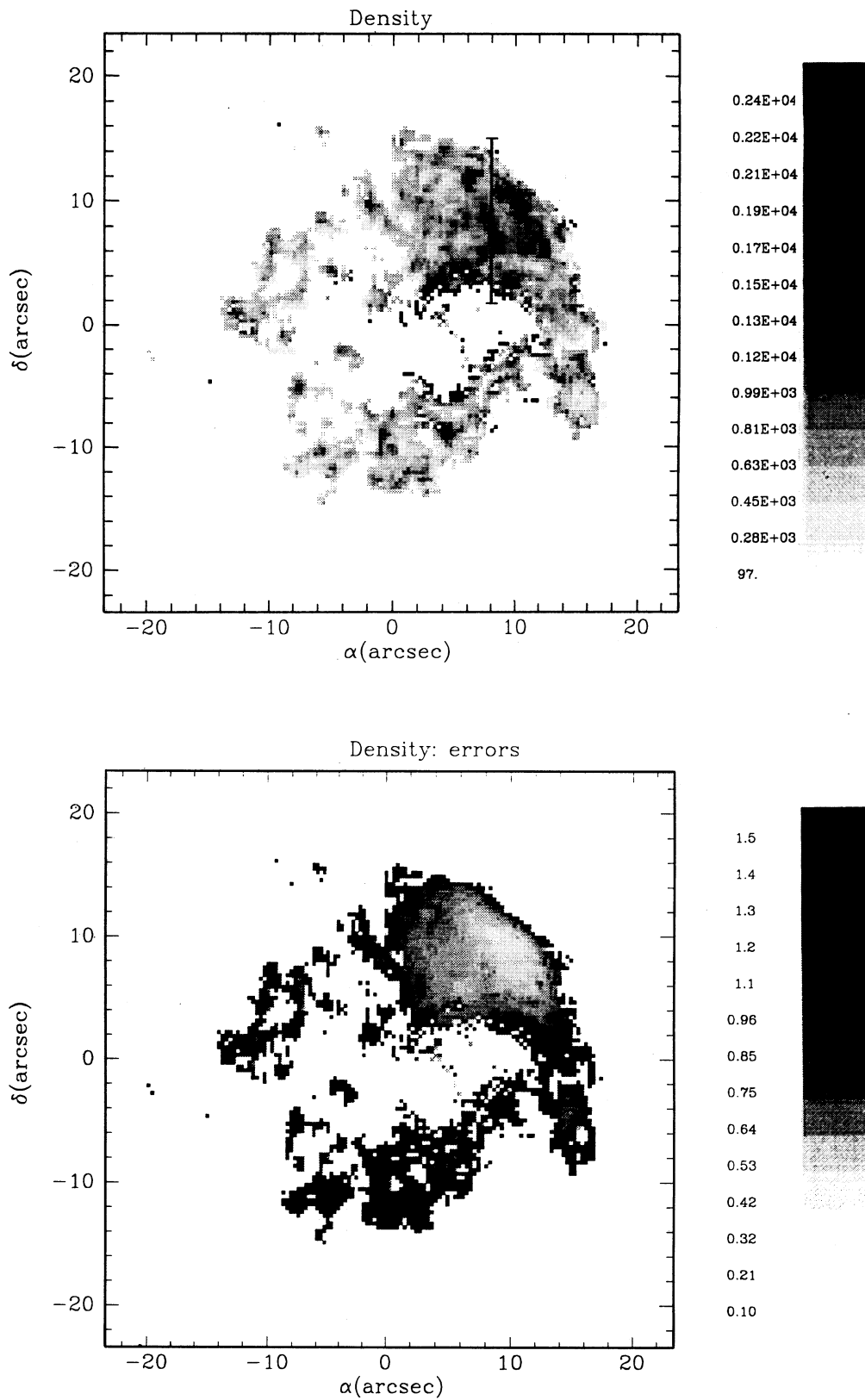


Fig. 5. (a) Density map of the western H II region. The density scale is shown to the right. (b) Error map for the densi

could be propagating, the aforementioned criteria can be applied unequivocally in order to establish the nature of this object. The western H II region is used to assay the conclusions.

The $H\alpha/[N II]$ image, shown in Figure 2a, indicates that this ratio is approximately equal to 7.5 in GGD 25 and 10 in the H II region. For $H\alpha/[S II]$ (Figure 2b) the values are 8.5 and 4 respectively. Scans for these ratios across both regions, their position shown in Figure 2a, are presented in Figures 3a and 3b for GGD 25 and 4a and 4b for the H II region. In both regions the line ratio seems to increase towards the edges. This effect is probably spurious, since errors are also larger near the edges due to a smaller signal to noise ratio, as can be seen from the scans in the equivalent error images. It is important to note that the line ratios found for the western H II region are in accordance to expectations, indicating a reasonable absolute accuracy for these images.

A first conclusion to be obtained from both ratios is that they clearly indicate that GGD 25 is not a Herbig-Haro object. Secondly, we can discard the possibility that GGD 25 is in some way connected to the western H II region, since the values taken by the line ratios, in particular $H\alpha/[S II]$, are different in both objects. Thus, it can be firmly established that GGD 25 is part of a different H II region, quite possibly, as proposed by Rodríguez, Cantó, & Moran (1988), of NGC 6334 A.

c) Density

A map of the electron density and the associated errors in the western H II region is presented in Figure 5. It was obtained in the manner described above. A scan of this image, its position shown in Figure 5a, is presented in Figure 6. In this case errors arising from an uncertain sky background are at least 30%. A mean electron density of 1000 cm^{-3} is found throughout the region, with knots where it is 2 to 3 times above the mean (see Figure 6). If this H II region is part of the NGC 6334 complex, at a distance of 1.7 kpc (Neckel 1978) its diameter is nearly 0.3 pc, and a mass of roughly 0.5 solar masses is inferred. This is a rather small value, but certainly not unique.

Unfortunately it was impossible to obtain an equivalent map for GGD 25 because of insufficient counts. For the few regions where a sufficient signal to noise ratio was attained, a minimum electron density of 2500 cm^{-3} was found. This conclusion is consistent with an image taken at $[S II] 6717 \text{ \AA}$, sensitive to densities smaller than 1000 cm^{-3} , where GGD 25 is very faint.

IV. CONCLUSIONS

- i) Direct images of GGD 25 taken with filters

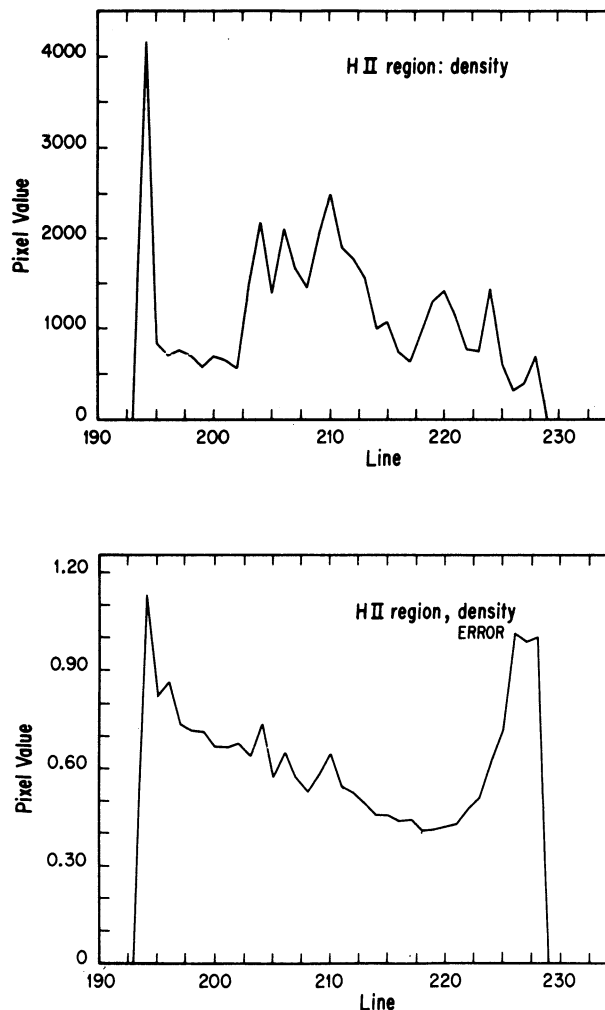


Fig. 6. Scan across the density map for the western H II region. In spite of the errors, shown below, a knotty appearance can be recognized. The scan position is shown in Figure 5a.

centered at $H\alpha$, $[N II]$ and $[S II]$ prove that this object is part of an H II region, quite probably NGC 6334 A, as first suggested by Rodríguez, Cantó, & Moran (1987). GGD 25 is very prominent in the I band. Polarimetric observations should determine whether this is due to reflection or *in situ* emission.

- ii) A density map of the H II region located to the west of GGD 25 shows that the region has a mean electron density of 1000 cm^{-3} , with knots that stand out 2-3 times above their surroundings. To a first approximation the region contains some 0.5 solar masses.

- iii) The mean electron density in GGD 25 is larger than about 2500 cm^{-3} .

iv) The H α frame of the region revealed that source number 8 of Harvey, Hyland, & Straw (1987), positioned at $\alpha = 17^h 16^m 57.4^s$ $\delta = -35^\circ 52' 10''$ (1950), is an emission line star.

I am grateful for the suggestions from an unknown referee, to L. Salas for his help with graphics presentations and to R. Papritz for her patience.

REFERENCES

- Bohigas, J. 1991, Reporte Técnico No. 92, Inst. de Astronomía, UNAM
- Gyulbugadhian, A.L., Glushkov, Yu.I., & Denisyuk, E.K. 1978, ApJ, 224, L137
- Hartmann, L., & Raymond, J.C. 1984, ApJ, 276, 560
- Harvey, P.M., & Gatley, I. 1983, ApJ, 269, 613
- Harvey, P.M., Hyland, A.R., & Straw, S.M. 1987, ApJ, 317, 173
- Jackson, J.M., Ho, P.T.P., & Haschick, A.D. 1988, ApJ, 333, L73
- McBreen, B., Fazio, G.G., Stier, M., & Wright E.L. 1979, ApJ, 232, L183
- McCall, M.L. 1984, MNRAS, 208, 253
- Moran, J.M., & Rodríguez, L.F. 1980, ApJ, 236, L159
- Neckel, T. 1978, A&A, 69, 51
- Persi, P., & Ferrari-Toniolo, M. 1982, A&A, 112, 292
- Rodríguez, L.F., Cantó, & J., Moran, J.N. 1982, ApJ, 255, 103
- _____. 1988, ApJ, 333, 801
- Straw, S.M., Hyland, A.R., & McGregor, P.J. 1989, ApJS, 69, 99

Joaquín Bohigas: Instituto de Astronomía, UNAM, Apartado Postal 877, 22860 Ensenada, B.C., México.